FIGURE 2.1

Schematic representation of the hydrologic cycle.

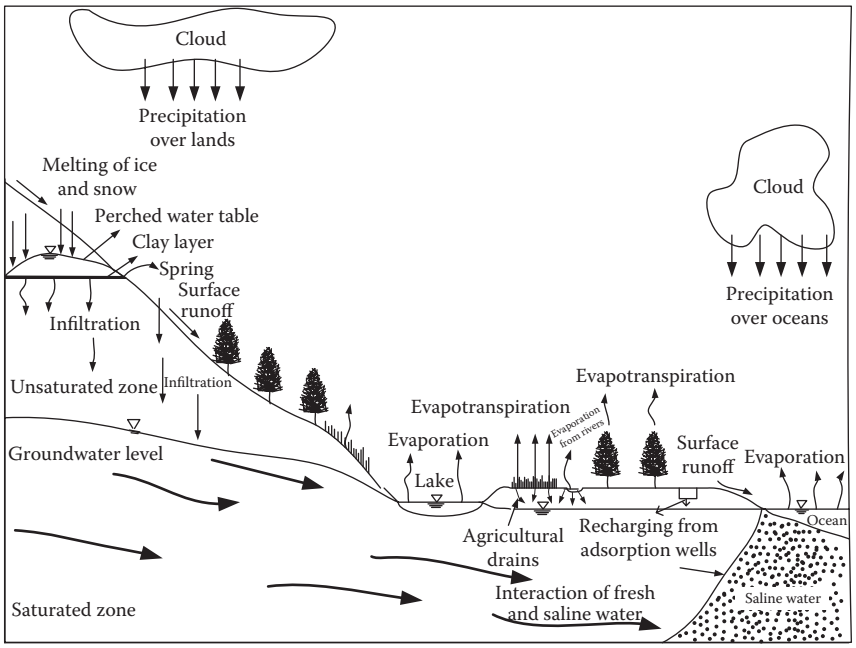

FIGURE 2.2

Classification of subsurface waters in a hypothetical section.

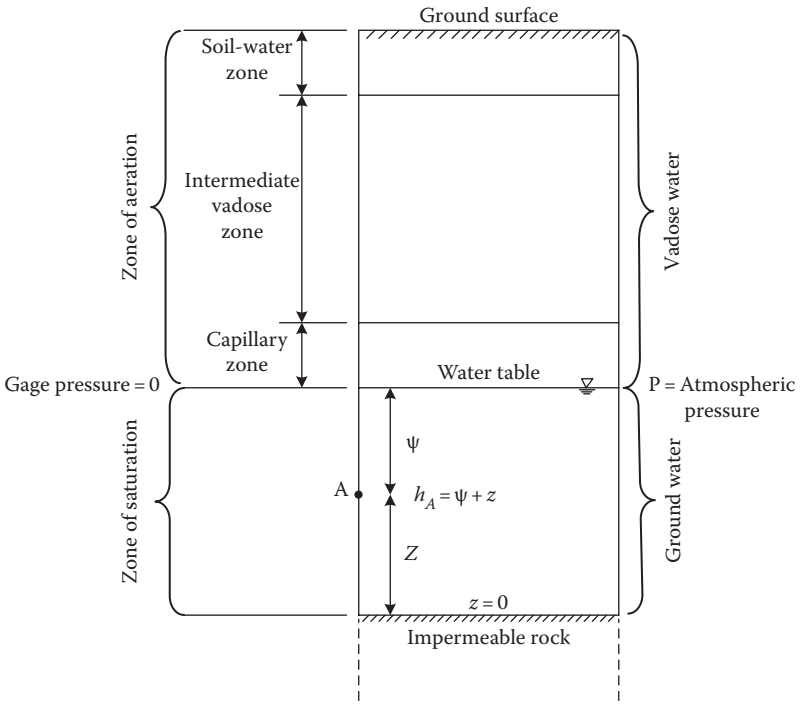

FIGURE 2.3

A schematic of capillary rise.

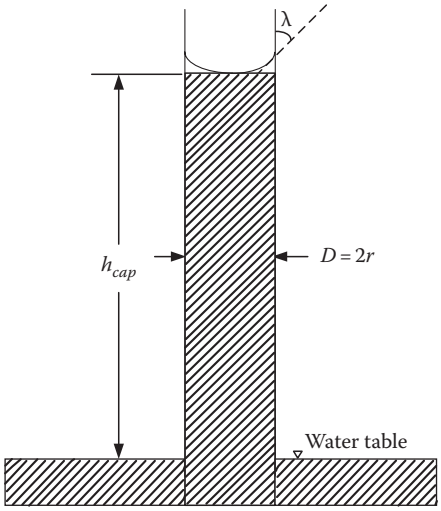

FIGURE 2.4

Schematic cross section illustrating unconfined and confined aquifers.

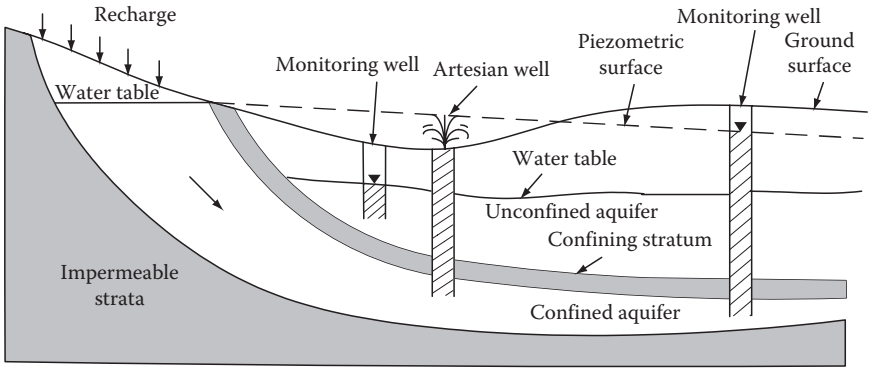

FIGURE 2.5

Total stress, effective stress, and fluid pressure on an arbitrary plane through a saturated porous medium.

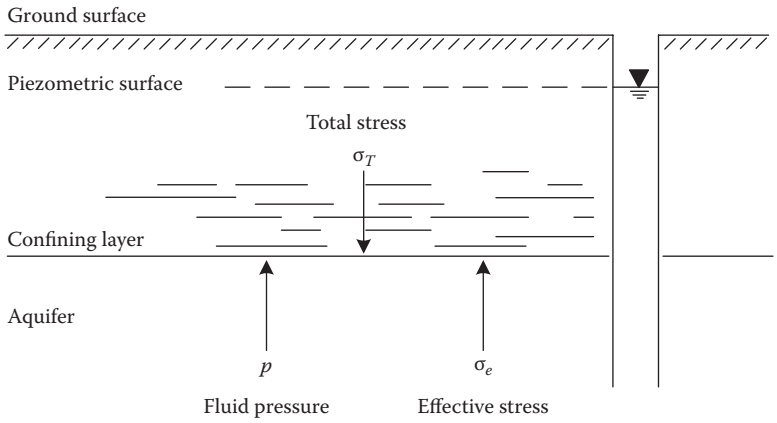

FIGURE 2.6

(a) Laboratory loading cell for the determination of soil compressibility. (b) Change of effective stress relative to void ratio. (c) Impact of repeated loading and unloading on effective stress. (d) Schematic curves of void ratio versus effective stress for clay and sand. (From Freeze, R. and Cherry, J., *Groundwater*, Prentice-Hall, Englewood Cliffs, NJ, 1979.)

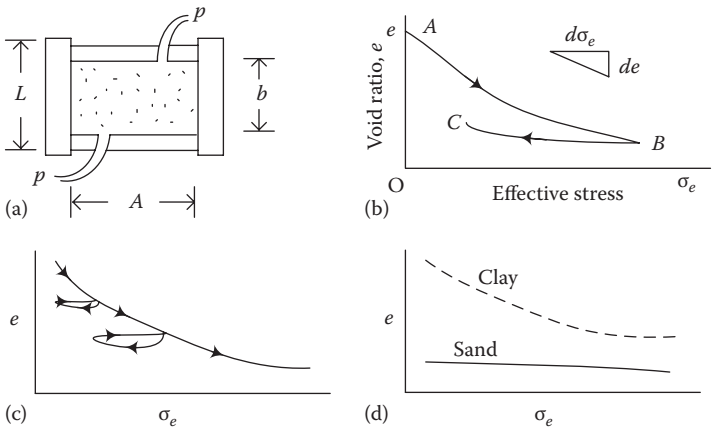

FIGURE 2.7

Land subsidence caused by groundwater pumping.

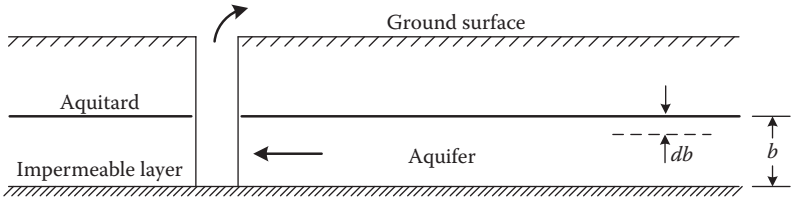

FIGURE 2.8

(a) Well-graded sedimentary deposit, with porous pebbles. (b) Poorly graded sedimentary deposit. (c) Well-graded sedimentary deposit with mineral filling. (d) Rock rendered porous by solution and fracturing.

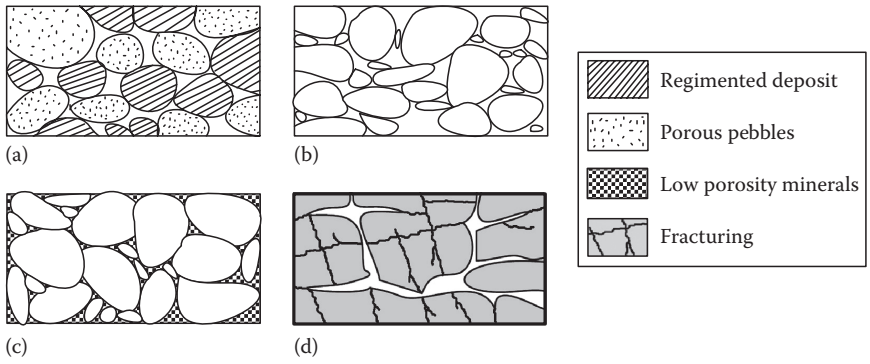

FIGURE 2.9

A schematic for defining storage coefficients of (a) confined and (b) unconfined aquifers.

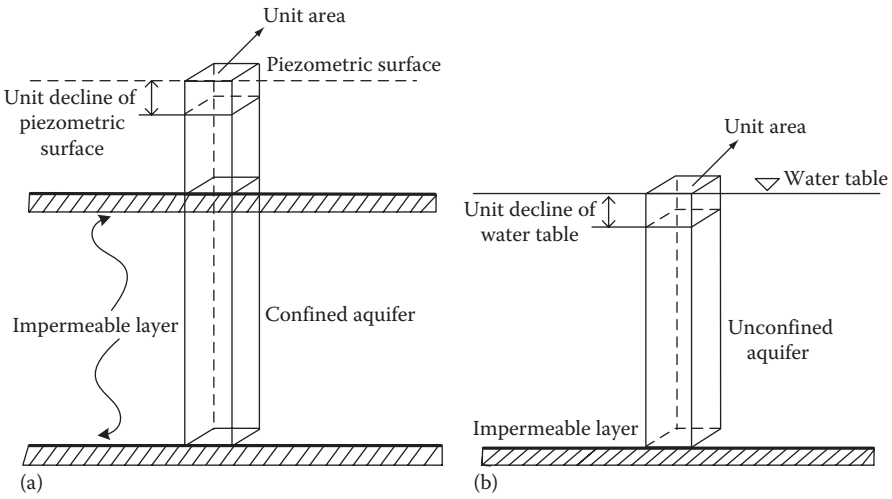

FIGURE 2.10

Movement of water in the zone of aeration by lowering the water table. (a) Water content above the water table. (b) Specific yield as a function of the time of drainage. (From Todd, D.K. and Mays, L.M., *Groundwater Hydrology*, John Wiley & Sons, Inc., New York, 2005.)

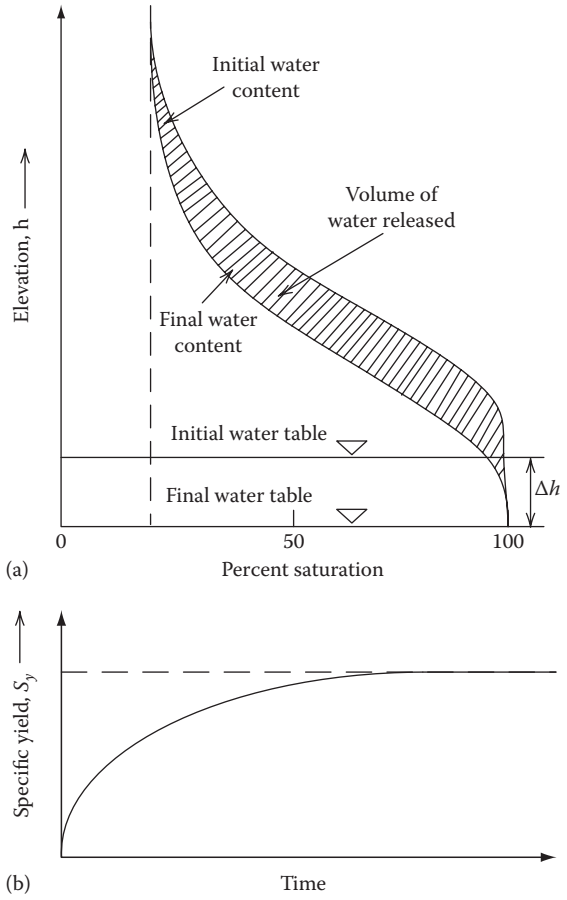

FIGURE 2.11

Heterogeneous karst aquifer system. (From Goldsheider, N. and Drew, D., *Methods in Karst Hydrology*, Taylor & Francis Group, London, U.K., 2007; Hansch, C. and Leo, A., *Substitute Constants for Correlation Analysis in Chemistry and Biology*, John Wiley & Sons, Inc., New York, 1979.)